

Shock-induced melting of MgSiO₃ perovskite and implications for melts in Earth's lowermost mantle

Joseph A. Akins,¹ Sheng-Nian Luo,² Paul D. Asimow,¹ and Thomas J. Ahrens¹

Received 12 April 2004; revised 23 June 2004; accepted 2 July 2004; published 30 July 2004.

[1] New shock wave equation of state (EOS) data for enstatite and MgSiO₃ glass constrain the density change upon melting of Mg-silicate perovskite up to 200 GPa. The melt becomes denser than perovskite near the base of Earth's lower mantle. This inference is confirmed by shock temperature data suggesting a negative pressure-temperature slope along the melting curve at high pressure. Although melting of Earth's mantle involves multiple phases and chemical components, this implies that the partial melts invoked to explain anomalous seismic velocities in the lowermost mantle may be dynamically stable. *INDEX TERMS*: 3919 Mineral Physics: Equations of state; 3944 Mineral Physics: Shock wave experiments; 8124 Tectonophysics: Earth's interior—composition and state (1212). *Citation*: Akins, J. A., S.-N. Luo, P. D. Asimow, and T. J. Ahrens (2004), Shock-induced melting of MgSiO₃ perovskite and implications for melts in Earth's lowermost mantle, *Geophys. Res. Lett.*, 31, L14612, doi:10.1029/2004GL020237.

[2] The perovskite (*pv*) structure of (Mg, Fe)SiO₃ is considered to be the most abundant phase in the lower mantle, which makes its high-pressure, high-temperature behavior a matter of some interest. Of particular importance, given seismic ultra-low velocity zones (ULVZs) [Williams and Garnero, 1996] above the core-mantle boundary, are constraints on the phase relations and density contrasts among mantle solids, mantle melts, and the core that may explain the presence and stability of partial melting at the very base of the mantle [Montague and Kellogg, 2000; Namiki, 2003; Zhong and Hager, 2003].

[3] The thermal EOS of MgSiO₃ *pv* has been constrained by numerous static experiments and computational studies [Wang et al., 1994; Utsumi et al., 1995; Funamori et al., 1996; Saxena et al., 1999; Fiquet et al., 2000; Karki et al., 2001; Marton et al., 2001; Brodholt et al., 2002]. Previous dynamic pressure-density-internal energy (*P*- ρ -*E*) data for MgSiO₃ composition are compiled in Marsh [1980] and Simakov and Trunin [1973]. We obtained new *P*- ρ -*E* Hugoniot data to 206 GPa on initial MgSiO₃ synthetic glass and natural Sri Lankan enstatite (*en*) (Table 1 of auxiliary material (electronic data supplement (EDS))¹) [Akins, 2003]. Interpretation of these data are complemented by our recent shock temperature (*T*) results to 180 GPa [Luo et al., 2004]. Shock *T* constrains the thermal EOS of

the high-*P* phases and can also indicate melting, since shock *T* in melts is typically lower than the extrapolation of solid Hugoniot. Here we compare the melting behavior of MgSiO₃ on the Hugoniot of three starting materials: an ultraporos equimolar mixture of MgO+SiO₂ (starting density $\rho_0 = 1.58 \text{ g/cm}^3$) [Marsh, 1980], MgSiO₃ glass ($\rho_0 = 2.73 \text{ g/cm}^3$) and *en* ($\rho_0 = 3.22 \text{ g/cm}^3$). We also combine diamond-anvil cell (DAC) and shock *T* data to define the melting curve of MgSiO₃ *pv* to 200 GPa and to examine the relative buoyancy of solids and melt of this composition.

[4] The phase in the shock state is not determined in most shock wave experiments. Whether fully-ordered crystalline high-pressure phases (H.P.P.) form during shock compression remains unknown but the advent of ultrafast x-ray [d'Almeida and Gupta, 2000] and electron [Siwick et al., 2003] diffraction promises to resolve this issue soon. For now, interpretation of shock data is guided by calculations of theoretical Hugoniot curves for candidate H.P.P. based on a Mie-Grüneisen offset from 3rd order Birch-Murnaghan isentropes (details are given in EDS and by McQueen et al. [1963]). Selected elastic and thermodynamic parameters of MgSiO₃ akimotoite, *pv*, and melt with low-pressure properties (L.P.P. melt) are listed in Table 2 of the EDS. Many Hugoniot data can be assigned to one of these phases, but the highest-*P* experiments on *en* require a new phase or a drastic change in EOS. Although an orthorhombic (*Cmcm*) postperovskite phase ~ 1.0 – 1.5% denser than *pv* has been reported [Murakami et al., 2004; Shim et al., 2004] (calculated thermodynamic parameters in EDS Table 2 from T. Tsuchiya et al. (Phase transition in MgSiO₃ perovskite in the Earth's lower mantle, submitted to *Science*, 2004, hereinafter referred to as Tsuchiya et al., submitted manuscript, 2004)), it is not dense enough to explain the highest-*P* data; we argue that these require a H.P.P. melt even denser than postperovskite. We estimate the parameters of a candidate EOS for this melt consistent with our data: $\rho_0 = 3.68 \text{ g cm}^{-3}$; $K_{oS} = 125 \text{ GPa}$; $K'_S = 4.0$; $\gamma = 2.4(V/V_0)^{1.0}$; $E_r = 2.4 \text{ MJ/kg}$ relative to *en*; and $C_V = 0.92 * 3nR$, where *R* is the gas constant.

[5] Consider first the Hugoniot data for ultraporos MgO+SiO₂ (Figure 1a) [Marsh, 1980]. Up to 21 GPa the density is similar to the Hugoniot of normal *en* [Simakov and Trunin, 1973; Marsh, 1980]. The datum at 31 GPa and 4.2 g/cm^3 , however, is substantially denser than the crystal Hugoniot. Calculations of possible H.P.P. indicate a reasonable fit for *pv*; other possibilities (e.g., periclase plus stishovite) cannot account for the density. We presume that conversion to *pv* is kinetically easier along the high-*T* porous-material compression path. The estimated shock *T*

¹Division of Geological and Planetary Sciences, California Institute of Technology, Pasadena, California, USA.

²Plasma Physics, Los Alamos National Laboratory, Los Alamos, New Mexico, USA.

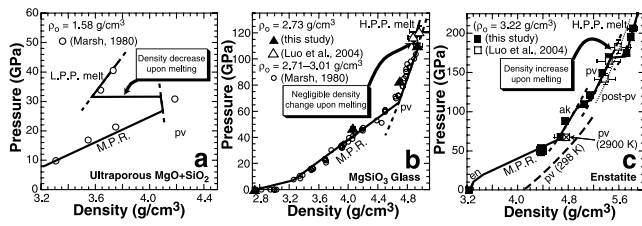


Figure 1. P - ρ plots of Hugoniot data and theoretical Hugoniot calculations for three starting materials of MgSiO₃ composition. Filled symbols use shock travel times by streak camera (this study); open symbols use radiance duration in shock temperature experiments [Luo et al., 2004]; small open circles from Marsh [1980]. (a) Ultraporous MgO+SiO₂. Calculated Hugoniot segments are shown for this starting material converting to candidate phases perovskite (pv) and low-pressure phase (L.P.P.) melt. Segments interpreted to contain multiple phases are labeled mixed-phase regime (M.P.R.). Note negative density change on melting at 32 GPa. (b) MgSiO₃ glass. Calculated Hugoniot segments are for glass converting to pv and to H.P.P. melt as well as M.P.R. between en and H.P.P. assemblages. Change in density on melting at 110 GPa is negligible. (c) Enstatite crystal. Calculated Hugoniot segments are for enstatite (en) and for conversion to akimotoite (ak), pv , and H.P.P. melt as well as suitable M.P.R. segments. The dotted curve is a calculation of the Hugoniot for en converting to the newly reported post-perovskite phase [Murakami et al., 2004; Shim et al., 2004; Tsuchiya et al., submitted manuscript, 2004]. Static data on the EOS of pv [Fiquet et al., 2000] are shown for reference. Note positive density change on melting at 170 GPa.

at 31 GPa, 4000 K, is above the melting curve of MgSiO₃ (Figure 2), but superheated solid shock states are common for shocks that overdrive the melting curve by less than $\sim 30\%$ [Luo and Ahrens, 2003]. The next datum, at 34 GPa, exhibits an abrupt decrease in density of $\sim 10\%$ that we propose is due to melting [Akins, 2003]. A calculated Hugoniot for ultraporous MgO+SiO₂ shocked to L.P.P. melt (EDS Table 2) agrees with the P - ρ data at 34 and 41 GPa (Figure 1a). The calculated T at 34 GPa, 4000 K, is an upper bound on the melting curve (Figure 2). At ~ 34 GPa, therefore, MgSiO₃ pv melts with a large positive ΔV_m to a low-density liquid presumably dominated by four-fold coordination of silicon.

[6] The MgSiO₃ glass data show a different behavior. Our 47 GPa point and existing data on ceramic materials of similar ρ_0 [Marsh, 1980] are consistent with a mixed phase region (M.P.R.) of en and H.P.P., perhaps mostly majorite. Our 87 and 110 GPa data are consistent with solid pv (Figure 1b). The lower-precision P - ρ estimates from time-resolved shock T experiments at 117 and 121 GPa [Luo et al., 2004] suggest density perhaps slightly lower than the extrapolation of the pv Hugoniot, but the difference is within error. However, the measured shock T at 117 GPa is ~ 1000 K lower than the calculated T for MgSiO₃ glass shocked to pv (Figure 2). Our interpretation is that the MgSiO₃ glass yields superheated pv up to 110 GPa and 6200 K followed by melting with negligible ΔV_m and a T drop of ~ 700 K to a dense melt by 117 GPa.

[7] The en crystal Hugoniot follows a still lower- T path and displays a third melting behavior (Figure 1c). First, the data at 68 and 88 GPa are too dense to still be en and show a steep slope consistent with a single-phase regime, yet are not dense enough to be pv (compare to the higher density of a laser-heated DAC XRD measurement on pv at 2900 K and 67 GPa [Fiquet et al., 2000], ~ 1300 K hotter than the shock state at 68 GPa). After examining all candidate phases, we conclude that akimotoite is attained between 70 and 90 GPa on the en Hugoniot [Akins, 2003]. At 110 to 150 GPa the calculated Hugoniot for en going to pv fits the data. The data between 57 and 140 GPa of Gong et al. [2004] on slightly porous natural orthopyroxene with Mg/(Mg+Fe) = 0.92 also show densities consistent with pv ; no akimotoite regime can be seen in their data, perhaps due to experimental scatter, initial porosity, or differences in phase relations due to Fe.

[8] At 170 GPa our en data show a jump in density of $\sim 5\%$. Figure 1c includes a calculated Hugoniot for conversion to the postperovskite solid [Murakami et al., 2004; Shim et al., 2004; Tsuchiya et al., submitted manuscript,

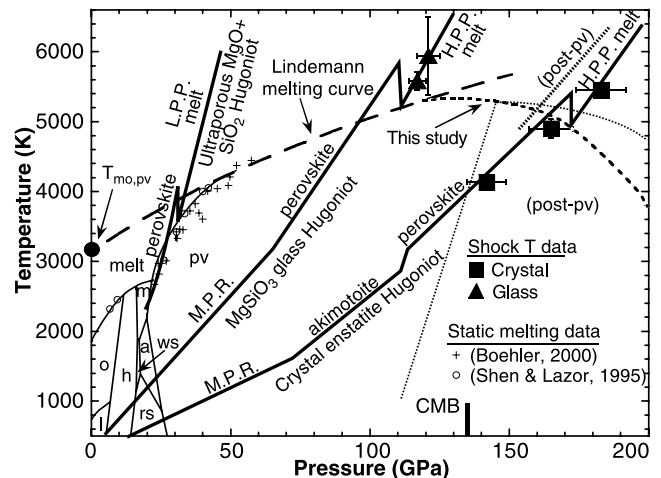


Figure 2. Proposed phase diagram of MgSiO₃ system with Hugoniot temperature data for glass and en [Luo et al., 2004]; shock temperature calculations for ultraporous mixture of MgO/SiO₂, MgSiO₃ glass and en ; and proposed pv melting curve. Phase assignments along the Hugoniot are the same as in Figure 1. Heavy dotted line shows calculated temperatures for en -to-postperovskite solid (Tsuchiya et al., submitted manuscript, 2004). Melting data from Boehler [2000] and Shen and Lazor [1995], constrain the light solid segment of the melting curve. The long-dashed curve is a Lindemann fit (see text). The short-dashed extrapolation accounts for the negative ΔV_m at 170 GPa. l : low clinoenstatite; o : orthoenstatite; h : high clinoenstatite; rs : ringwoodite + stishovite; ws : wadsleyite + stishovite; m : majorite. Phase boundaries to 30 GPa from Presnall [1995] except: m - ak - pv triple point [Hirose et al., 2001]; m -L.P.P. melt- pv triple point [Ito and Katsura, 1992]. Protoenstatite field not shown. CMB shows P of core-mantle boundary. Proposed boundary between pv and postperovskite from Tsuchiya et al. (submitted manuscript, 2004) and schematic melting curve of postperovskite phase are shown as light dotted lines.

2004], but this explains only about half the density jump observed. A similar jump is observed along the quartz Hugoniot at 115 GPa. In the SiO₂ system this corresponds to a drop in longitudinal sound speed to the bulk sound velocity [Chhabildas and Miller, 1985; McQueen, 1991] and a 2000 K drop in T [McQueen and Fritz, 1982; Lyzenga et al., 1983; Boslough, 1988]. In SiO₂ these observations demand a transition from superheated solid to high-density liquid. We propose that the *en* Hugoniot undergoes a similar transition at 170 GPa from *pv* solid to H.P.P. melt with an increase in density [Akins, 2003]. The P - ρ data inferred from radiance duration in shock T experiments [Luo et al., 2004] are consistent with this interpretation within their error bars. Moreover, the shock T measured at 142 and 165 GPa is within error of calculated T along the *en*-to-*pv* Hugoniot, whereas the T datum at 183 GPa is at least 500 K below the calculation, which again suggests a melt as the H.P.P. (Figure 2). Calculated shock T for *en*-to-postperovskite phase (Tsuchiya et al., submitted manuscript, 2004) at 183 GPa does not fit the data (Figure 2). However, definitive confirmation that the *en* Hugoniot passes into a dense melt rather than a dense solid will require longitudinal sound speed measurements across the transition.

[9] Because the H.P.P. melt Hugoniot state is at lower T than the superheated extrapolation of the *en*-to-*pv* Hugoniot, it is necessary to examine how much of the 5% density jump along the Hugoniot is due to T rather than the ΔV_m between melt and solid on the melting curve. In order for ΔV_m to be positive, a 5% increase in *pv* density upon cooling from the extension of the *pv* Hugoniot to the H.P.P. melt Hugoniot requires a thermal expansion coefficient ($\alpha \geq 6.0 \times 10^{-5} \text{ K}^{-1}$) [Akins, 2003]. Fiquet et al. [2000] provide thermal EOS data for *pv* with $\alpha = 2.7 \times 10^{-5} \text{ K}^{-1}$ at 5000 K and room P ; fitting their data to an Anderson-Grüneisen form [Anderson, 1995] yields a predicted $\alpha = 1.0 \times 10^{-5} \text{ K}^{-1}$ at 170 GPa. With this value and a ΔT of -730 K from comparison of our *pv* and H.P.P. melt Hugoniot we find that ΔV_m is indeed negative and that the melt is 3.2% denser than the solid on the melting curve at 170 GPa and 5000 K (details in EDS, Table 3).

[10] For a univariant reaction such as the congruent melting of a pure phase, the volume change of the reaction is related to its slope in P - T space by the Clausius-Clapeyron equation,

$$dT/dP = \Delta V_m / \Delta S_m, \quad (1)$$

where ΔS_m is entropy of fusion. ΔS_m should be positive and a weak function of P , even if disorder contributes somewhat to the entropy of shocked solids. Hence the slope of the melting curve is roughly proportional to ΔV_m and, in particular, $\Delta V_m < 0$ implies a negative slope. The shock T data of [Luo et al., 2004], which place the melting curve at 5500 K at 110 GPa and 5000 K at 170 GPa, are therefore consistent with the negative ΔV_m that our EOS data require at 170 GPa.

[11] At 32 GPa, where we observe a $\sim 10\%$ increase in volume along the Hugoniot upon melting of ultraporous MgO+SiO₂, the melting curve of *pv* is directly constrained by multianvil and DAC studies. It has a slope of 50 K/GPa, which is consistent with the ΔV_m and ΔS_m between our derived equations of state for L.P.P. melt and *pv*. We fitted

the melting curve of *pv* in the H.P.P. regime to a Lindemann law [Anderson, 1995],

$$T_m = T_{mo} \left(\frac{\rho_o}{\rho} \right)^{2/3} \exp \left\{ \frac{2\gamma_o}{q} \left[1 - \left(\frac{\rho_o}{\rho} \right)^q \right] \right\}, \quad (2)$$

where the volume dependence of the Grüneisen parameter of *pv* is constrained by static high- T EOS and shock data and the fictive melting T of *pv* to H.P.P. melt at zero P , T_{mo} , is a free parameter. Choosing $T_{mo} = 3100 \text{ K}$ results in a curve that merges with the upper end of the DAC melting points [Shen and Lazor, 1995; Sweeney and Heinz, 1998; Boehler, 2000] around 50 GPa and agrees with the melting T at 110 GPa inferred from shock data. The Lindemann melting curve slope of 10 K/GPa at 110 GPa and a ΔV_m of $+0.8\%$ estimated from our shock EOS data on MgSiO₃ glass leads to $\Delta S_m = 0.4R$. If this value applies also at 170 GPa, then our inferred ΔV_m of -3.2% implies that the slope of the melting curve should be -35 K/GPa at 170 GPa (Figure 2). We estimate that melting of MgSiO₃ *pv* at the core-mantle boundary, 135 GPa, occurs at $T = 5300 \text{ K}$, a volume change of -0.2% and a Clapeyron slope of -3 K/GPa . If the postperovskite phase is stable on the liquidus at these conditions, T will be slightly higher and the volume change and Clapeyron slope will be positive; however, the positive Clapeyron slope suggested for the *pv*-postperovskite phase boundary suggests that even if the adiabatic geotherm crosses into the postperovskite field at the top of D'' , the base of the conductive core-mantle boundary layer may be hot enough to cross back into the *pv* stability field.

[12] In conclusion, shock wave EOS data on various phases of MgSiO₃, supplemented by shock T measurements [Luo et al., 2004], suggest that MgSiO₃ melt increases substantially in density with increasing P across the *pv* stability field. The initially very steep slope of the melting curve seen in DAC experiments is consistent with a low-density melt similar in structure to that seen at ambient P , but by $\sim 120 \text{ GPa}$ the melt approaches the density of solid *pv*. Although this H.P.P. melt must be dominated by six-fold coordination, its compressibility remains larger than that of *pv* and by 170 GPa the melt exceeds the density of *pv*. This result by itself is insufficient to describe the dynamics of the lowermost mantle, where other components are significant contributors. However, the existence of a melt denser than the most abundant dense silicate is provocative. It suggests that small degree partial melts may be neutrally buoyant and stable for long times in the D'' layer, and that silicate melts may also accumulate to high degrees of melting just above the core mantle boundary and explain the existence of ULVZs. The implications for chemical evolution of the mantle, the dynamics and chemical signatures of deep mantle plumes, and possible ongoing interactions between core and mantle remain areas for further work.

[13] **Acknowledgments.** This work was funded by the National Science Foundation through grants EAR-9903806 and EAR-0207934. Thanks to Carl Francis and Stephen Mackwell for providing the high quality Sri Lankan enstatites used in this study. The authors thank an anonymous reviewer and editor Kristine Larson for their help improving the manuscript. This is Caltech GPS contribution #9046.

References

Akins, J. A. (2003), Dynamic compression of minerals in the MgO-FeO-SiO₂ system, Ph.D. thesis, Calif. Inst. of Technol., Pasadena.

- Anderson, O. L. (1995), *Equations of State of Solids for Geophysics and Ceramic Sciences*, 405 pp., Oxford Univ. Press, New York.
- Boehler, R. (2000), High-pressure experiments and the phase diagram of lower mantle and core materials, *Rev. Geophys.*, *38*, 221–245.
- Boslough, M. B. (1988), Postshock temperatures in silica, *J. Geophys. Res.*, *93*, 6477–6484.
- Brodholt, J. P., A. R. Oganov, and G. D. Price (2002), Computational mineral physics and the physical properties of perovskite, *Philos. Trans. R. Soc. London, Ser. A*, *360*(1800), 2507–2520.
- Chhabildas, L. C., and J. M. Miller (1985), Release-adiabat measurements in crystalline quartz, *Rep. SAND85-1092*, Sandia Natl. Lab., Albuquerque, N. M.
- d'Almeida, T., and Y. M. Gupta (2000), Real-time x-ray diffraction measurements of the phase transition in KCl shocked along 100, *Phys. Rev. Lett.*, *85*(2), 330–333.
- Fiquet, G., A. Dewaele, D. Andrault et al. (2000), Thermoelastic properties and crystal structure of MgSiO₃ perovskite at lower mantle pressure and temperature conditions, *Geophys. Res. Lett.*, *27*, 21–24.
- Funamori, N., T. Yagi, W. Utsumi et al. (1996), Thermoelastic properties of MgSiO₃ perovskite determined by in situ X ray observations up to 30 GPa and 3000 K, *J. Geophys. Res.*, *101*, 8257–8269.
- Gong, Z. Z., Y. W. Fei, F. Dai et al. (2004), Equation of state and phase stability of mantle perovskite up to 140 GPa shock pressure and its geophysical implications, *Geophys. Res. Lett.*, *31*, L04614, doi:10.1029/2003GL019132.
- Hirose, K., T. Komabayashi, M. Murakami, and K.-I. Funakoshi (2001), In situ measurements of the majorite-akimotoite-perovskite phase transition boundaries in MgSiO₃, *Geophys. Res. Lett.*, *28*, 4351–4354.
- Ito, E., and T. Katsura (1992), Melting of ferromagnesian silicates under the lower mantle conditions, in *High Pressure Research: Application to Earth and Planetary Sciences*, *Geophys. Monogr. Ser.*, vol. 67, edited by Y. Syono and M. H. Manghnani, pp. 315–322, AGU, Washington, D. C.
- Karki, B. B., L. Stixrude, and R. M. Wentzcovitch (2001), High-pressure elastic properties of major materials of Earth's mantle from first principles, *Rev. Geophys.*, *39*, 507–534.
- Luo, S. N., and T. J. Ahrens (2003), Superheating systematics of crystalline solids, *Appl. Phys. Lett.*, *82*(12), 1836–1838.
- Luo, S. N., J. A. Akins, T. J. Ahrens, and P. D. Asimow (2004), Shock-compressed MgSiO₃ glass, enstatite, olivine and quartz: Optical emission, temperatures, and melting, *J. Geophys. Res.*, *109*, B05205, doi:10.1029/2003JB002860.
- Lyzenga, G. A., T. J. Ahrens, and A. C. Mitchell (1983), Shock temperatures of SiO₂ and their geophysical implications, *J. Geophys. Res.*, *88*, 2431–2444.
- Marsh, S. P. (1980), *LASL Shock Hugoniot Data*, 658 pp., Univ. of Calif. Press, Berkeley.
- Marton, F. C., J. Ita, and R. E. Cohen (2001), Pressure-volume-temperature equation of state of MgSiO₃ perovskite from molecular dynamics and constraints on lower mantle composition, *J. Geophys. Res.*, *106*, 8615–8627.
- McQueen, R. G. (1991), The velocity of sound behind strong shocks in SiO₂, in *Shock Compression of Condensed Matter 1991*, edited by S. C. Schmidt et al., pp. 75–78, Elsevier Sci., New York.
- McQueen, R. G., and J. N. Fritz (1982), Some techniques and results from high-pressure shock-wave experiments utilizing the radiation from shocked transparent materials, in *Shock Waves in Condensed Matter 1981*, edited by W. J. Nellis, L. Seaman, and R. A. Graham, pp. 193–207, Am. Inst. of Phys., New York.
- McQueen, R. G., J. N. Fritz, and S. P. Marsh (1963), On the equation of state of stishovite, *J. Geophys. Res.*, *68*, 2319–2322.
- Montague, N. L., and L. H. Kellogg (2000), Numerical models of a dense layer at the base of the mantle and implications for the geodynamics of D^{''}, *J. Geophys. Res.*, *105*, 11,101–11,114.
- Murakami, M., K. Hirose, K. Kawamura et al. (2004), Post-perovskite phase transition in MgSiO₃, *Science*, *304*(5672), 855–858.
- Namiki, A. (2003), Can the mantle entrain D^{''}?, *J. Geophys. Res.*, *108*(B10), 2487, doi:10.1029/2002JB002315.
- Presnall, D. C. (1995), Phase diagrams of Earth-forming minerals, in *Mineral Physics and Crystallography: A Handbook of Physical Constants*, *AGU Ref. Shelf*, vol. 2, edited by T. J. Ahrens, pp. 248–268, AGU, Washington D. C.
- Saxena, S. K., L. S. Dubrovinsky, F. Tutti, and T. Le Bihan (1999), Equation of state of MgSiO₃ with the perovskite structure based on experimental measurement, *Am. Mineral.*, *84*(3), 226–232.
- Shen, G. Y., and P. Lazor (1995), Measurement of melting temperatures of some minerals under lower mantle pressures, *J. Geophys. Res.*, *100*, 17,699–17,713.
- Shim, S. H., T. S. Duffy, R. Jeanloz, and G. Shen (2004), Stability and crystal structure of MgSiO₃ perovskite to the core-mantle boundary, *Geophys. Res. Lett.*, *31*, L10603, doi:10.1029/2004GL019639.
- Simakov, G. V., and R. F. Trunin (1973), On the existence of the overdense perovskite structures in magnesian silicates under conditions of high pressure, *Izv. Earth Phys.*, *9*, 603–604.
- Siwick, B. J., J. R. Dwyer, R. E. Jordan, and R. J. D. Miller (2003), An atomic-level view of melting using femtosecond electron diffraction, *Science*, *302*(5649), 1382–1385.
- Sweeney, J. S., and D. L. Heinz (1998), Laser-heating through a diamond-anvil cell: Melting at high pressures, in *Properties of Earth and Planetary Materials at High Pressure and Temperature*, *Geophys. Monogr. Ser.*, vol. 101, edited by M. H. Manghnani and T. Yagi, pp. 197–213, AGU, Washington, D. C.
- Utsumi, W., N. Funamori, T. Yagi et al. (1995), Thermal expansivity of MgSiO₃ perovskite under high pressures up to 20 GPa, *Geophys. Res. Lett.*, *22*, 1005–1008.
- Wang, Y. B., D. J. Weidner, R. C. Liebermann, and Y. S. Zhao (1994), P-V-T equation of state of (Mg, Fe)SiO₃ perovskite—Constraints on composition of the lower mantle, *Phys. Earth. Planet. Inter.*, *83*(1), 13–40.
- Williams, Q., and E. J. Garnero (1996), Seismic evidence for partial melt at the base of Earth's mantle, *Science*, *273*(5281), 1528–1530.
- Zhong, S., and B. H. Hager (2003), Entrapment of a dense layer by thermal plumes, *Geophys. J. Int.*, *154*, 666–676.

T. J. Ahrens, J. A. Akins, and P. D. Asimow, Division of Geological and Planetary Sciences, Mail Code 170-25, California Institute of Technology, Pasadena, CA 91125, USA. (asimow@gps.caltech.edu)

S.-N. Luo, Plasma Physics P-24, MS E526, Los Alamos National Laboratory, Los Alamos, NM 87545, USA.